The frozen blowup profile of the Okamoto, Sakajo and Wunsch family: a control variate for its spectral exponent

Munawar Kazmi
Independent researcher
munawarkazmi.com
munawarsaeedkazmi1@gmail.com

August 15, 2026

Abstract

On the circle, the one parameter family of Okamoto, Sakajo and Wunsch admits, above a critical advection $a_c = 0.6890665\ldots$, a blowup whose spatial scale neither shrinks nor expands, $\omega = f(x)/(T-t)$. This frozen profile was found numerically by Lushnikov, Silantyev and Siegel, and its existence and nonlinear stability near $a = 1$ were proved by Chen. Its Fourier spectrum decays algebraically, $\left|\hat{f}_k\right| \sim k^{-\beta}$, because a high order derivative of f jumps at the stagnation point antipodal to the singularity, and β has been obtained by least squares fits to the spectrum.

This note is about determining β accurately. The local exponent at a stagnation point is $\mu = (c-1)/(ac)$, with c the Hilbert transform of f there, and $\beta = \mu + 1$; this relation is due to Chen, and at the stagnation point where f has a simple zero it closes as $c = 1/(1-a)$, a normalisation identity used throughout this literature. Reading c off a discrete profile is the difficulty: across seven resolutions the value at the singular stagnation point wanders by 2×10^{-2} with no monotone trend, so extrapolation in N returns noise. Our observation is that the two constants are read from the same profile and carry the same discretisation error, and that one of them is known exactly. Regressing the unknown constant against the known one across resolutions and evaluating at the exact value cancels the error without requiring its size or its rate, collapsing the spread by a factor of 800.

This yields β to five digits. At $a = 0.8$ we obtain $\beta = 3.0024227 \pm 4.6 \times 10^{-6}$, which excludes the value 3 by five hundred times the scatter, and β varies continuously with a rather than locking to an integer. At $a = 0.71$ we obtain $\beta = 9.29546$ against the published fitted value 9.32592, a correction of 0.33 percent, the two determinations sharing no machinery.

We add three smaller numerical results. The linearisation about the profile in renormalised time has exactly two eigenvalues outside the open left half plane, both forced by symmetry, giving linear stability modulo those symmetries at $a = 0.8$, well away from the neighbourhood of $a = 1$ where nonlinear stability is proved. The profile equation admits a first integral, and integrating it around the circle gives the global constraint PV $\oint \mathrm{d}y/U = 0$, which we verify to 10^{-12}. Finally, at $a = 1/2$, where the model is exactly solvable, the datum $\omega_0 = \sin x$ blows up at $T = \pi$ exactly.

1 Introduction

The question of whether solutions of the three dimensional incompressible Euler equations can develop singularities from smooth data remains open, and the same question for Navier and Stokes is one of the Clay Millennium Prize problems. A recurring strategy is to study one dimensional models which retain the competition between vortex stretching and transport while discarding the geometry.

Constantin, Lax and Majda [1] introduced the model

$$\omega_t = \omega \mathcal{H} \omega, \tag{1}$$

where $\mathcal{H}$ is the Hilbert transform, and solved it in closed form. De Gregorio [2] restored the transport term, and Okamoto, Sakajo and Wunsch [3] embedded both in the one parameter family

$$\omega_t + a\, u\, \omega_x = \omega\, u_x, \qquad u_x = \mathcal{H}\omega, \tag{2}$$

posed here on the circle with u of zero mean. The parameter a tunes the strength of transport against stretching. At $a = 0$ transport is absent and (2) reduces to (1); at $a = 1$ the two terms are in genuine competition, and this case is understood to be critical. Jia, Stewart and Šverák [4] studied the ground state of the De Gregorio model, Lei, Liu and Ren [5] proved global regularity on the circle for data of one sign, and Chen, Hou and Huang [6] proved finite time blowup on the line for data of low Hölder regularity. The broader programme of computer assisted singularity detection in fluid equations is exemplified by Luo and Hou [7], Elgindi [8] and Chen and Hou [9].

Two features of (2) make it a good testbed. Both endpoints of the family are known exactly, which makes every numerical statement checkable, and the solution structure is simple enough that the blowup profile can be computed directly rather than inferred from a diverging simulation.

Relation to existing work. Self similar blowup for this family is under active study and the present results must be read against it.

The pole dynamics line. The closest work to this paper is a body of results obtained by complex singularity and pole dynamics methods, and it already contains much of the setting used here. Lushnikov, Silantyev and Siegel [19] sweep a on both the real line and the circle with high precision spectral simulations and a nonlinear eigenvalue solve. They locate the critical advection $a_c = 0.6890665337007457\ldots$ at which the width exponent c_l vanishes; they identify, for $a_c < a \lesssim 0.95$ on the circle, the frozen blowup $\omega = f(x)/(T-t)$ which is the object of this paper, and compute its profile for $a_c < a \le 0.85$; they observe that f has a jump in a high order derivative at $x = \pm\pi$, antipodal to the singularity, which at $a = 0.8$ is a jump in f''; and they measure the resulting algebraic spectral decay, reporting its exponent as p_b, which is our β. Their Theorem 1 gives the exponent $\gamma = 1/(1-a)$ of the leading complex singularity, from the balance $a\gamma = \gamma - 1$, which is the same algebra as Proposition 8 applied to a different object. We claim none of this, and the regime diagram of Section 4 should be read as reproducing theirs rather than as establishing it.

The frozen profile is not only observed but proved. Chen [17] constructs it: for a in a neighbourhood of 1 he proves that (2) on the circle admits a self similar solution $\omega = \omega_a(x)/(1+c_\omega t)$ with an odd profile and no spatial rescaling, which is $c_l = 0$, and in a companion theorem that it is nonlinearly stable and attracts smooth data. The same theorem states the local exponent at the singular stagnation point, which is (11) below, and the regularity that follows from it, namely that the profile is C^1 but not $C^{1,\alpha}$ there. Existence, stability, exponent and regularity for the object of this paper are therefore all his, in the regime $a \to 1^-$.

What this paper adds is neither the setting nor the local relations but the determination of the constant they leave open. The exponent β has been obtained by least squares fits to the spectrum, which we show in Section 9 is accurate to about a percent and biased; the control variate developed there returns five digits, and it works at $a \approx 0.8$, away from the $a \to 1^-$ neighbourhood in which [17] controls the profile.

Silantyev, Lushnikov, Siegel and Ambrose [20] construct exact pole dynamics solutions on the circle for $a = 0$ and $a = 1/2$; Section 8 is an application of theirs and claims no more. Xu [21] studies the spectrum of the linearisation about the collapse profile at $a = 0$ on the real line, obtaining the essential spectrum, a point spectrum $\{0, 1\}$ consisting of symmetry modes, and a spectral gap. His Section 2 records the general self similar profile equation (12), and in the course of his Section 4 he derives $\mathcal{H}\Omega(0) = (1+c_l)/(1-a)$, which is (14) below; Proposition 7 is therefore his, obtained independently here, and we retain it only because Proposition 6 needs it. Our Section 6 asks his question for the frozen profile on the circle, where the second symmetry mode is translation rather than dilation, and answers it numerically where he answers it with proof.

Okamoto, Sakajo and Wunsch [3] study global existence against blowup using a criterion in the spirit of Beale, Kato and Majda together with energy estimates, and do not consider self similar profiles. They do fit the spectrum in the combined form $|\hat{\omega}_n| \sim Cn^{-p}e^{-\delta n}$ and track both parameters in time, observing that $\delta(t)$ decays exponentially, which they read as evidence of smoothness for all time, while $p(t)$ decreases monotonically and, in their words, they are unable to see its asymptotic value from the numerical data. The exponent β of (15) is the analogue of that p for a frozen blowup profile, and (15) determines it in closed form given one local quantity.

Huang, Tong and Wei [11] construct infinitely many compactly supported self similar blowup solutions of the De Gregorio model on the real line, organised as eigenfunctions of a compact operator and as solutions of nonlinear eigenvalue problems, with profiles in $H_0^1 \cap H^2$ and smooth in the interior of the support. Huang, Tong and Wang [16] study self similar blowup of the generalised model from data with derivative degeneracy, reporting one scale blowup with regular profiles for $a > 0$ against a two scale scenario with singular outer profile for $a \le 0$, and constructing an explicit family of singular profiles in the latter regime. Both use the standard self similar ansatz, whose profile equation $(c_l x + au)\omega_x = (c_\omega + u_x)\omega$ reduces to (7) at $c_l = 0$, $c_\omega = -1$. We claim no novelty for that formulation.

Huang, Qin, Wang and Wei [12] prove that the family admits exact self similar blowup with interiorly smooth profiles for all $a \le 1$, obtained as a fixed point of an a dependent nonlinear map, with characterisations of regularity, monotonicity and far field decay. Their profiles fail to be smooth only at the boundary of a compact support, whereas the profile here is $C^{1,1}$ at an *interior* point. The two are consistent, and the reason is the domain: on the circle U has zero mean by construction, so it must change sign and interior stagnation points are forced, while on the line they are not. Their analogues of c_1 and c_2 are defined as integrals and bounded rather than evaluated, for instance $2\eta/\pi \le c(f) \le 4/\pi$, and no closed form appears.

Huang, Qin and Wang [13] construct blowups with two collapsing spatial scales on the line, one measuring the distance to the blowup point and one the shrinking bulk. Those profiles narrow, $c_l > 0$, so they belong to the narrowing regime of Section 4 rather than the frozen one, and the blowup there occurs where ω_0 vanishes with $\mathcal{H}\omega_0 > 0$ rather than at a zero of the velocity.

Guo and Jiu [15] study stability on the torus at $a = 1$ near the excited state $-\sin 2\theta$, proving linear and nonlinear instability for a broad class of data. That is the steady state analogue, at the critical parameter, of the observation that the higher members of Proposition 4 are not generic attractors. It concerns equilibria rather than blowup profiles and takes no renormalised time limit.

Zheng [14] constructs exactly self similar C^α blowup for the generalised De Gregorio equation at small $|a\alpha|$, again on the line and again narrowing, with rescaling factor $(1-t)^{1+\lambda(a)}$.

A pattern runs through the constructive part of this literature. With the exception of [19] and [20], every construction we are aware of works on the real line with a narrowing profile, $c_l \neq 0$. The circle behaves differently for a reason that is not a matter of taste: there U has zero mean by construction, so it must change sign, interior stagnation points are forced, and by Proposition 6 the profile cannot be smooth at them. That is the setting in which a frozen profile, $c_l = 0$, becomes the attractor, and it is the setting [19] already works in.

What remains to be done there is the local analysis at those stagnation points. Proposition 6 at the *singular* stagnation point, where f has no simple zero and $\mu \neq 1$, is the part that none of these references contains, and it is what turns the fitted exponent of [19] into a predicted one. The parity statement fixing the two stagnation points π apart, the control variate of Section 9, the first integral and global constraint of Section 10, and the linear stability computation of Section 6 are likewise not in them. Two numerical coincidences with [16] invited closer comparison, and Proposition 7 is what makes that comparison possible, since it puts both settings in one formula.

The transition near $a \approx 0.75$. [16] identifies $a^{c,2} \approx 0.751$ as the value at which its self similar profile *loses* stability as a increases. The frozen profile studied here *gains* selection as a increases through roughly the same value. These are not the same object: their profiles carry $c_l \neq 0$ and therefore narrow, which in the language of Section 4 places them in the narrowing regime, whereas a frozen profile requires $c_l = 0$ exactly. It is tempting to read the two as complementary halves of one exchange of stability, in which the narrowing attractor gives way to the frozen one.

Table 2 tests that reading. The mechanism survives and the location does not.

The mechanism: c_l falls smoothly to zero rather than jumping, so the narrowing branch merges with the frozen one rather than being replaced by it, which is the right shape for an exchange.

The location: an earlier version of this paper read Table 2 as giving $c_l = 0.004536 \pm 0.000543$ at $a = 0.751$, eight standard errors from zero, and concluded $a_c \gtrsim 0.795$. That is withdrawn, and it was wrong. The critical advection is known to far better precision than anything measured here: [19] obtains $a_c = 0.6890665337007457\ldots$ from a nonlinear eigenvalue problem, and [21] recomputes the branch independently by Newton continuation, finding its zero crossing at 0.6888, in agreement to 0.04 percent.

The failure is one of resolution, and it is visible in Table 2 itself once the published branch is put beside it: 1.058 against 1.0000 at $a = 0$, 0.748 against 0.7474 at $a = 0.2$, 0.512 against 0.4809 at $a = 0.4$, 0.325 against the exact $1/3$ at $a = 0.5$, and 0.179 against 0.1691 at $a = 0.6$. A half width measurement carrying several percent of bias cannot resolve a quantity of size

0.0045, and fitting $c_l = A(a_c - a)^p$ through it, with the best a_c running from 0.795 at $p = 2$ to 0.844 at $p = 4.5$, was an extrapolation through convex data of exactly the kind warned against in Section 9.

An independent check from this paper agrees with the published value rather than with the withdrawn one. [19] reports the spectral exponent diverging as $a \to a_c^+$, and β as determined in Section 9 does the same, taking the values 16.362, 9.295, 6.795 and 4.213 at $a = 0.70, 0.71, 0.72, 0.75$. Extrapolating $1/\beta$ linearly to zero from the two closest pairs gives 0.6868 and 0.6828, with the pair nearer the transition giving the larger value, consistent with $a_c = 0.68907$ and not with 0.795. We quote this loosely, since $1/\beta$ is convex and this is the same trap once more, but its direction is not in doubt.

The coincidence with [16] therefore stands unresolved rather than refuted, and our earlier reason for refuting it was itself an artefact. Their $a^{c,2} \approx 0.751$ is a stability boundary for a profile on the line, while $a_c = 0.68907$ is where the width exponent vanishes on the circle. The two numbers are close and describe different events, and nothing established here decides whether they are related.

The constant $1/(1-a)$. This identity is not a result of the present work and appears in four places in this literature, generally as a normalisation rather than as a theorem. [17] fixes the time rescaling by imposing $c_\omega(t) = (a-1)u_x(t,0)$, which at $c_\omega = -1$ is Proposition 8. [16] states the general form in its equation (2.10), $c_l = c_\omega + (1-a)U_X(0)$, which rearranges to Proposition 7. [21] states that same general form as $\mathcal{H}\Omega(0) = (1+c_l)/(1-a)$. And Theorem 1 of [19] reaches $\gamma = 1/(1-a)$ for the power of the leading complex singularity from the balance $a\gamma = \gamma - 1$, identical in form to the $ac = c - 1$ of Proposition 8, though the object is a power at a complex singularity rather than a value of $\mathcal{H}f$ at a real stagnation point.

An earlier version of this paper compared Proposition 8 only against Theorem 2.6 of [16], an exact solution for $a < 0$ with $\mu = 1/(1-a)$, and concluded the resemblance was superficial on the grounds that their μ is an exponent while ours is a value of $\mathcal{H}f$. That comparison was aimed at the wrong part of the paper: equation (2.10) of the same reference is the relation itself. We record the error because it is the kind that a reader checking one theorem rather than the whole paper will repeat.

Our contributions are as follows.

1. *The control variate, and β to five digits.* The two stagnation point constants are read from the same discrete profile and carry the same error, and one of them is known exactly. Regressing one against the other across resolutions and evaluating at the exact value collapses the spread by a factor of 800, giving $\beta = 3.0024227 \pm 4.6 \times 10^{-6}$ at $a = 0.8$ and excluding $\beta = 3$ (Section 9).

2. *A correction to the published exponent.* At $a = 0.71$ the same determination gives $\beta = 9.29546$ against the fitted 9.32592 of [19], a difference of 0.33 percent between two methods sharing no machinery (Remark 11).

3. *The linear spectrum at $a = 0.8$.* Exactly two eigenvalues lie outside the open left half plane, both forced by symmetry, so the profile is linearly stable modulo those symmetries. This is numerical, and it sits well away from the neighbourhood of $a = 1$ in which [17] proves nonlinear stability (Section 6).

4. *A first integral and a global constraint.* The profile equation integrates in closed form on any interval free of zeros of U, and integrating once around the circle forces PV $\oint \mathrm{d}y/U = 0$, verified to 10^{-12} (Section 10).

5. *The blowup time at $a = 1/2$.* Specialising the exact solution of [20] to $\omega_0 = \sin x$ gives $T = \pi$ exactly (Section 8).

The remaining sections are supporting numerics rather than claims: Section 4 recovers the regime picture of [19] with an independent diagnostic and records where our resolution falls short of theirs, and Section 5 treats the profile equation as a fixed point of the evolution nonlinearity and checks the amplitude it fixes against simulation to 10^{-5}.

Throughout, the initial datum is $\omega_0 = \sin x$. This is not a generic choice, and Section 11 records what that costs.

2 The model and its exactly known endpoints

Write ω for the vorticity on the circle $x \in [0, 2\pi)$ and let $\mathcal{H}$ denote the Hilbert transform, acting on Fourier modes as $\widehat{\mathcal{H}\omega}_k = -i\,\mathrm{sgn}(k)\,\hat{\omega}_k$. The velocity is recovered from $u_x = \mathcal{H}\omega$ with u of zero mean, so $\hat{u}_k = -\hat{\omega}_k/|k|$ for $k \neq 0$.

The case $a = 0$. Setting $z = \mathcal{H}\omega + i\omega$ converts (1) into the Riccati equation $z_t = z^2/2$, whence

$$\omega(x,t) = \frac{4\,\omega_0(x)}{\big(2 - t\,\mathcal{H}\omega_0(x)\big)^2 + t^2\omega_0(x)^2}. \tag{3}$$

For $\omega_0 = \sin x$ the denominator collapses to $4 + 4t\cos x + t^2$ and

$$\|\omega(t)\|_\infty = \frac{4}{4 - t^2}, \tag{4}$$

so the blowup time is $T = 2$ and the rate exponent is exactly one.

The case $a = 1$. For $\omega_0 = \sin x$ one has $\mathcal{H}\omega_0 = -\cos x$ and $u = -\sin x$, so $u\omega_x = \omega u_x$ pointwise and $\sin x$ is a steady state. Hence $T = \infty$.

The family therefore runs between a case whose blowup time is exactly 2 and a case whose blowup time is exactly infinite, and any numerical scheme can be calibrated against both.

3 Numerical method

Space is treated pseudospectrally: products are formed on an equispaced grid of N points, dealiased by the two thirds rule, with the Nyquist mode set to zero. Time stepping is classical fourth order Runge and Kutta, with the step governed by two constraints. Accuracy near blowup requires $\Delta t = \mathrm{cfl}/\max(\|u_x\|_\infty, \|\omega\|_\infty)$, since the stretching term drives the growth. Stability requires $\Delta t < c_{\mathrm{adv}}/(k_{\mathrm{cut}}\,|a|\,\|u\|_\infty)$, because the transport term has eigenvalues on the imaginary axis out to $i\,a\,u\,k_{\mathrm{cut}}$ and the method is stable there only to 2.828.

Two diagnostics require care. First, the supremum norm is computed from the spectral interpolant rather than the grid samples: the grid maximum errs by $O(\Delta x^2 f'')$, and since the peak narrows like $1/\|\omega\|_\infty$ near blowup, that error grows precisely when it matters. We locate the peak by Newton iteration on $f'(x) = 0$ against the interpolant, at $O(N)$ cost for a single point. Second, spectral decay rates are measured over a band bounded away from both ends: the low wavenumber end is contaminated by the analytic factor multiplying the singular behaviour, and the high wavenumber end by the dealiasing mask. Section 9 quantifies both.

The implementation passes nineteen checks against closed forms and conserved quantities, including (3) and (4) to 2×10^{-11}, conservation of $\int \omega$ to 10^{-16} for $a \in \{0, \frac{1}{2}, 1, -\frac{1}{2}\}$, spatial convergence following the predicted analyticity strip across four orders of magnitude, and fourth order temporal convergence with measured ratios 16.65, 16.28, 16.16, 16.07.

4 Blowup times and two distinct regimes

From $\omega_0 = \sin x$ we observe finite time blowup for every $a < 1$, with rate exponent one throughout. Table 1 collects the blowup times, estimated by fitting $\omega/(\mathrm{d}\omega/\mathrm{d}t) = (T - t)/p$, a straight line in t with slope $-1/p$ and root T.

a	0	0.2	0.4	0.5	0.6	0.7	0.8	0.9	1
T	2 (exact)	2.3101	2.7858	π (exact)	3.6500	4.4641	6.0719	10.757	∞ (exact)
p	1 (exact)	0.997	1.000	1.001	1.001	0.999	1.000	1.049	n/a

Table 1: Blowup time and rate exponent from $\omega_0 = \sin x$. No transition to global existence appears below $a = 1$; instead T diverges as $a \to 1$.

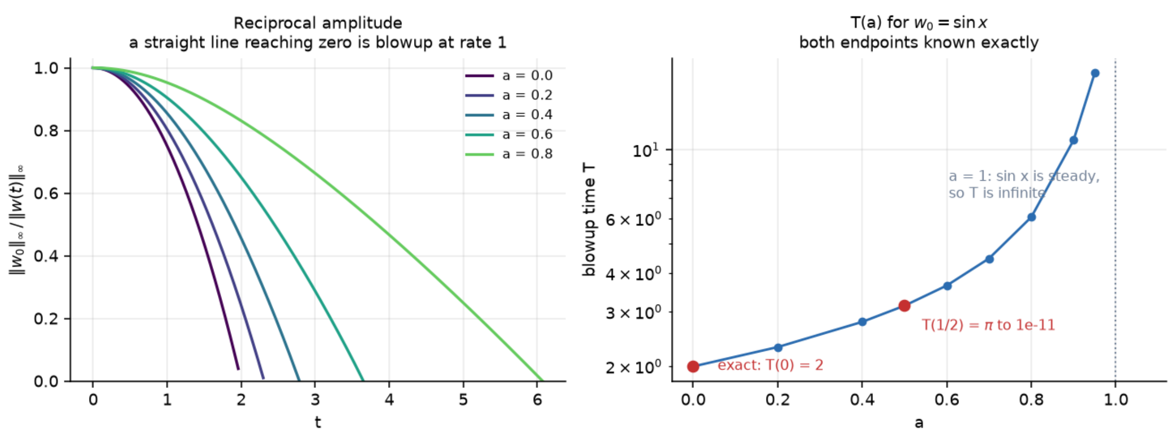

Figure 1: Left: reciprocal amplitude $\|\omega_0\|_\infty / \|\omega(t)\|_\infty$ for several values of a. A straight line reaching zero is blowup with rate exponent one. Right: the blowup time $T(a)$ from $\omega_0 = \sin x$, on a logarithmic scale. Both endpoints are known exactly, $T(0) = 2$ and $T(1) = \infty$, and the curve runs between them without any transition to global existence at intermediate a. The agreement of $T(1/2)$ with π is marked but unexplained.

Remark 1. The value at $a = 1/2$ agrees with π to 1.2×10^{-11} and continues to do so under refinement across an eightfold range in N. We have no explanation for this and record it as an observation.

The blowups are not all alike. Comparing normalised spectra $|\hat{\omega}_k| \,/\, \max_k |\hat{\omega}_k|$ at successive decades of amplitude growth gives a diagnostic which is invariant under translation and assumes nothing about the profile shape. At $a = 0.8$ the curves converge: successive deviations from the first snapshot are 3.30×10^{-3}, 3.68×10^{-3}, 3.76×10^{-3}, 3.78×10^{-3} across four decades of growth, the peak location locks to $x = 2.16699$, and the spectral tail remains at 2.7×10^{-17} throughout, so a grid of 4096 points carries an amplitude of 10^6 without strain. At $a = 0.4$ the same comparison moves by 0.72 over a single decade and resolution is exhausted by $\|\omega\|_\infty = 5.8\times10^3$.

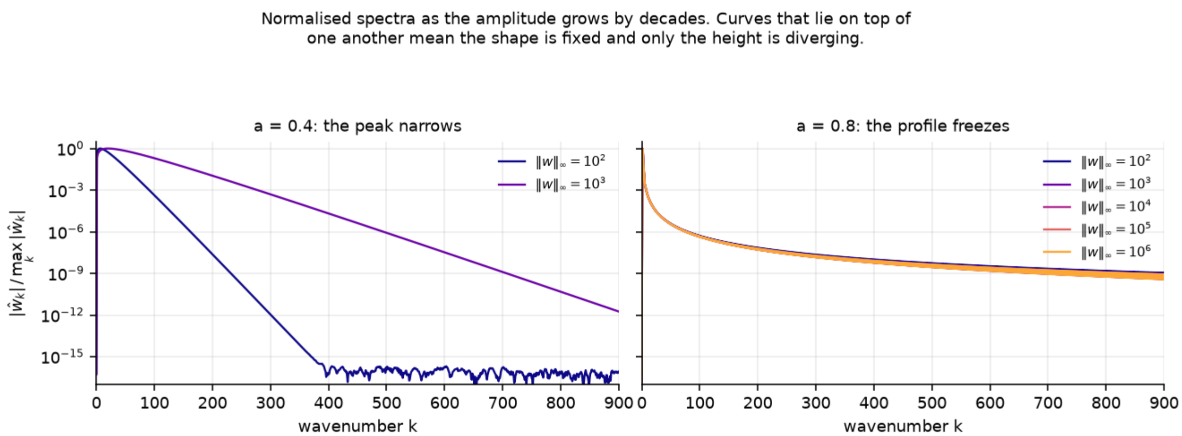

Figure 2: Normalised spectra $|\hat{\omega}_k| \,/\, \max_k |\hat{\omega}_k|$ at successive decades of amplitude growth. Taking the modulus removes the translation, so no alignment of the peaks is required and the comparison assumes nothing about the profile shape. Left, $a = 0.4$: the curves spread steadily as the peak narrows, and resolution is exhausted by $\|\omega\|_\infty = 5.8 \times 10^3$. Right, $a = 0.8$: five curves spanning four decades of growth lie on top of one another, so the shape is fixed and only the height diverges.

We refer to the first behaviour as a *frozen* profile and the second as *narrowing*, illustrated in Figure 2. Only the frozen case is analysed below.

The dichotomy is due to [19], who established it on the circle, located the transition at $a_c = 0.68906653370074 57\ldots$, and computed the width exponent to five to eight digits by a nonlinear eigenvalue solve. What this section reports is an independent measurement of the same quantity by a different and much cruder route, and it should be read as a check on our diagnostic rather than as a determination of theirs.

The distinction is quantitative. In the general self similar ansatz of Proposition 7, the peak width scales like $(T-t)^{c_l}$ while the amplitude grows like $(T-t)^{-1}$, so width $\sim$ amplitude$^{-c_l}$ and c_l is minus the slope of one against the other on logarithmic axes. A frozen profile is exactly $c_l = 0$. Measuring the width as the half width at half maximum around the peak, which is robust whether the spectrum is exponential or algebraic, gives Table 2. The method is calibrated at $a = 0$, where the exact solution (3) has width proportional to $(2-t)$ and amplitude $4/(4-t^2)$, so $c_l = 1$; the measurement returns 1.048. Against the published branch, Table 2 is accurate to a few percent and not of one sign; the introduction gives that comparison term by term, together with the estimate of a_c it forces us to withdraw.

Remark 2 (One signed data)**.** Lei, Liu and Ren [5] proved global regularity on the circle for data of one sign at $a = 1$. The mechanism appears to reach well below that. From

a	0	0.2	0.4	0.5	0.6
c_l	1.058	0.748	0.512	0.325	0.179
a	0.70	0.74	0.75	0.77	0.80
c_l	0.032321	0.007273	0.004536	0.001294	0.000398
std. err.	1.5×10^{-3}	7.5×10^{-4}	5.4×10^{-4}	3.0×10^{-4}	1.2×10^{-4}

Table 2: The spatial scaling exponent measured from the dynamics. The exact value at $a = 0$ is 1. The upper block is resolution limited and quoted to two figures; the lower block is fitted over three decades of amplitude, to 10^6. Values at $a \geq 0.78$ are omitted because they are not monotone in a at the 5×10^{-4} level, which is the true noise floor rather than the smaller figure the regression reports.

$\omega_0 = 1 - \cos x$, integrating to $t = 200$, the amplitude remains bounded at 2.72, 2.40 and 2.17 for $a = 0.7$, 0.8 and 0.9, while for $a = 0.6$ the solution reaches 10^6 by $t = 133$ and for $a = 0.5$ it exhausts resolution at 9.6×10^3. The threshold lies between 0.6 and 0.7. We record this as an observation; it says nothing about the frozen profile, which is reached from sign changing data.

5 The profile equation

Substituting the ansatz

$$\omega(x,t) = \frac{f(x - x_p)}{T - t} \tag{5}$$

into (2) gives $f/(T-t)^2$ on the left and $\mathcal{R}(f)/(T-t)^2$ on the right, where

$$\mathcal{R}(f) = f\,\mathcal{H}f - a\,U f', \qquad U' = \mathcal{H}f, \quad \textstyle\int U = 0 \tag{6}$$

is the same quadratic nonlinearity that drives the evolution. The profile equation is therefore the fixed point problem

$$\boxed{\mathcal{R}(f) = f.} \tag{7}$$

Proposition 3 (No free scaling). *If f solves (7) and $c \neq 1$, then cf does not.*

Proof. $\mathcal{R}$ is quadratic, so $\mathcal{R}(cf) = c^2\mathcal{R}(f) = c^2 f$, which equals cf only when $c^2 f = cf$, that is $c = 1$. □

Proposition 3 is what makes (7) useful rather than merely descriptive: unlike a linear eigenvalue problem it fixes the amplitude of f outright. Since (5) gives $\|\omega(t)\|_\infty = \|f\|_\infty/(T-t)$, we obtain the falsifiable prediction

$$\frac{\mathrm{d}}{\mathrm{d}t}\frac{1}{\|\omega\|_\infty} = -\frac{1}{\|f\|_\infty}. \tag{8}$$

The left side is measured by time marching the partial differential equation; the right side by Newton's method on an algebraic fixed point. The two share nothing but the value of a.

We solve (7) by Newton iteration, assembling the Jacobian one column at a time through the same masked transforms used to evaluate $\mathcal{R}$, and regularising the translation mode by a rank one shift along f'. At $a = 0.8$ the profile taken directly from the simulation satisfies (7) to 1.3×10^{-5} before Newton is applied; the iteration then converges quadratically, with residuals 1.35×10^{-5}, 4.07×10^{-11}, 1.77×10^{-12}. Table 3 compares the two sides of (8).

N	simulation, via (8)	profile equation	agreement
2048	4.148459148	4.148481857	5.5×10^{-6}
4096	4.154779433	4.154737187	1.0×10^{-5}

Table 3: $\|f\|_\infty$ at $a = 0.8$, computed two independent ways.

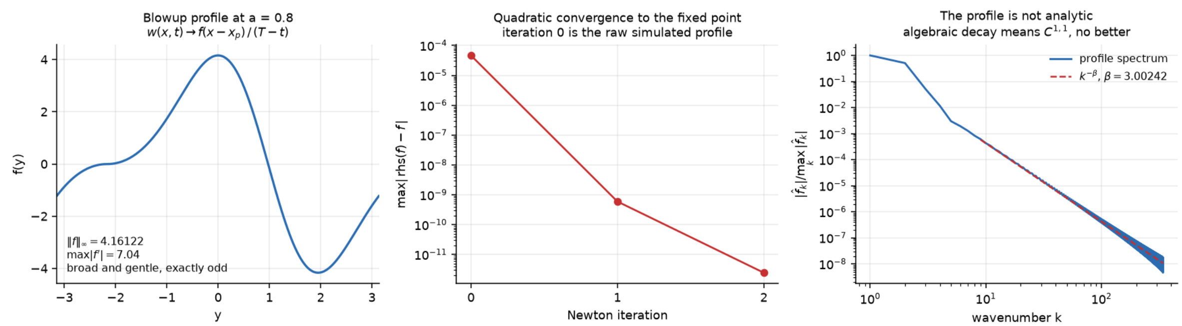

Figure 3: The blowup profile at $a = 0.8$. Left: $f(y)$, broad and gentle, with $\|f\|_\infty = 4.16$ against $\max|f'| = 7.04$, and exactly odd about each stagnation point. Centre: the Newton residual for (7), starting from the profile taken directly out of the simulation, which already satisfies the equation to 1.3×10^{-5}; convergence is quadratic. Right: the profile spectrum on logarithmic axes against $k^{-\beta}$ with $\beta = 3.00242$ from (15), the exponent predicted in Section 9 rather than fitted to this curve. The decay is algebraic, not exponential, so the profile is not analytic.

The shared value drifts by 1.5×10^{-3} between the two resolutions, which is not Newton finding different branches: re-solving at $N = 4096$ from the interpolated $N = 2048$ solution returns the same answer, and mapping it back down reproduces the $N = 2048$ value to 2×10^{-12}. Each grid has one solution and the simulation finds that grid's solution. The slow convergence is explained in Section 7: the profile is only $C^{1,1}$.

Proposition 4 (Dilation)**.** *If f solves (7) then so does $f(n\,\cdot)$ for every positive integer n, with the same $\|f\|_\infty$.*

Proof. The Hilbert transform commutes with integer dilation on the circle, so $\mathcal{H}[f(n\,\cdot)](x) = (\mathcal{H}f)(nx)$. Since the velocity is recovered by integrating $U' = \mathcal{H}f$, the velocity of $f(n\,\cdot)$ is $U(nx)/n$, while $\frac{\mathrm{d}}{\mathrm{d}x} f(nx) = nf'(nx)$. The two factors of n cancel in the advection term, so

$$\mathcal{R}\big(f(n\,\cdot)\big)(x) = f(nx)(\mathcal{H}f)(nx) - a\,\frac{U(nx)}{n}\,nf'(nx) = \big[f\,\mathcal{H}f - a\,U f'\big](nx) = f(nx). \qquad \square$$

So profiles come in families. The nth member carries $2n$ stagnation points spaced π/n, with exponents alternating between the two values of the base member, and $\|f\|_\infty$, c_1, c_2 and β are all unchanged. Numerically, $f(n\,\cdot)$ solves (7) to 10^{-11} for $n \le 4$, against 2×10^{-12} for the base profile itself.

Genericity. Every result here starts from $\omega_0 = \sin x$, which is the ground state of the $a = 1$ model and therefore not a generic datum. Proposition 5 and the stability computation of Section 6 predict that any datum in the basin converges to the same profile, and this is testable independently of them. At $a = 0.8$ and $N = 2048$:

datum	$\|f\|_\infty$	c_1	c_2	β
$\sin x$	4.1484819	4.996663	−1.6580199	3.003911
$\sin x + 0.3 \sin 2x$	4.1484819	4.996663	−1.6580199	3.003911
$\sin x + 0.5 \cos 2x - 0.2 \sin 3x$	4.1484819	4.996663	−1.6580199	3.003911
$\sin 3x + 0.4 \sin 4x$	4.1612203	5.006926	−1.668103	2.999354

Table 4: The same profile is reached from every datum tested. The first three agree to seven digits. The fourth lands on the $n = 2$ member of Proposition 4, which on a grid of 2048 points is represented as accurately as the base member on 1024 points, and indeed reproduces the $N = 1024$ values of Table 6 exactly.

Selection. Solutions of (7) exist over a wider range of a than the dynamics selects. Starting Newton from each simulation's own profile and recording the residual *before* the iteration begins gives an order parameter: it reads 0.33 to 0.56 for a between 0.3 and 0.6, then 0.19, 5.0×10^{-2}, 2.6×10^{-3}, 1.3×10^{-5} and 5.5×10^{-5} at $a = 0.65, 0.70, 0.75, 0.80, 0.85$. The frozen regime is therefore roughly $0.75 \leq a \leq 0.85$ at the amplitudes reached, degrading smoothly rather than switching off.

6 Linear stability in renormalised time

Set $s = -\log(T - t)$ and $W(y, s) = (T - t)\,\omega$. Then $\omega = e^s W$ and $\mathrm{d}s/\mathrm{d}t = e^s$, so $\omega_t = e^{2s}(W + W_s)$, while $\mathcal{R}$ is quadratic and gives $\mathcal{R}(\omega) = e^{2s}\mathcal{R}(W)$. The factors cancel and

$$W_s = \mathcal{R}(W) - W. \tag{9}$$

The profile is exactly a fixed point of (9), and the eigenvalues of $J = D[\mathcal{R}(\cdot) - \cdot](f)$ are growth rates in renormalised time.

Proposition 5 (Forced eigenvalues)**.** *$Jf = f$ and $Jf' = 0$.*

Proof. Since $\mathcal{R}$ is quadratic, its derivative satisfies $D\mathcal{R}(f)f = 2\mathcal{R}(f) = 2f$, so $Jf = D\mathcal{R}(f)f - f = f$. The second identity is translation invariance: $\mathcal{R}$ commutes with shifts, so differentiating $\mathcal{R}(f(\cdot + \epsilon)) = f(\cdot + \epsilon)$ at $\epsilon = 0$ gives $D\mathcal{R}(f)f' = f'$ and hence $Jf' = 0$. □

The eigenvalue 1 is not an instability. It reflects the freedom to shift the blowup time: replacing T by $T + \epsilon$ gives $W = f\tau/(\tau + \epsilon)$ with $\tau = T - t$, which to first order is $f - \epsilon e^s f$ and grows like e^s. The eigenvalue 0 is translation. Numerically, $\|Jf - f\|_\infty \,/\, \|f\|_\infty = 1.3 \times 10^{-12}$ and $\|Jf'\|_\infty \,/\, \|f'\|_\infty = 4.0 \times 10^{-11}$, so Proposition 5 also serves as a sharp check on the assembled Jacobian.

Every remaining eigenvalue at $a = 0.8$ lies in the open left half plane, at $N = 512$, 1024 and 2048 alike. The profile is therefore linearly stable up to the two symmetry directions, which is the precise sense in which the dynamics selects it, and is consistent with a simulation from $\sin x$ reaching it without tuning. The same test applied to profiles taken from simulations at $a = 0.65, 0.70, 0.75, 0.80$ returns stability in every case.

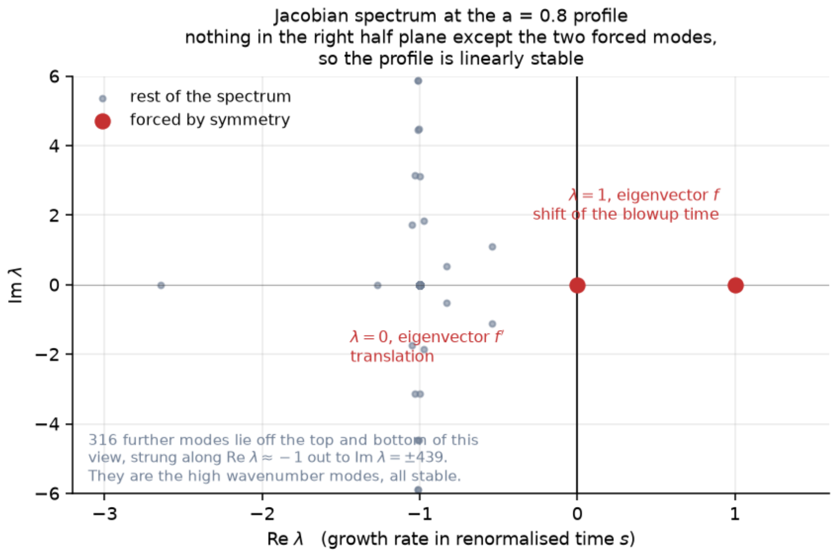

Figure 4: Spectrum of the linearisation (9) about the $a = 0.8$ profile, so that the abscissa is a growth rate in renormalised time s. The two marked eigenvalues are forced by symmetry, at 1 with eigenvector f (freedom to shift the blowup time) and at 0 with eigenvector f' (translation), both verified against Proposition 5 to 10^{-11} or better. Nothing else lies in the closed right half plane. The modes omitted from the view are the high wavenumber ones, strung along $\mathrm{Re}\,\lambda \approx -1$ and stable.

We note two limitations. The leading stable eigenvalue does not converge in N, taking values -0.54, -0.146, -0.41 at $N = 512, 1024, 2048$, so the rate of approach to the profile is not determined here, only its sign. At $a = 0.85$ and $N = 1024$ the Newton solve lands on a different branch, with $\|f\|_\infty = 6.249$ and an unstable eigenvalue at $+2.077$, whereas at $N = 2048$ the same value of a yields $\|f\|_\infty = 5.668$ matching its simulation to 8×10^{-6}. Continuation in a jumps branches outright. The branch structure is real and we have not mapped it.

7 Stagnation points and the local exponent

This section is background. The relations recalled here are due to [17] and [21], and the closed form at a simple zero is a normalisation identity used throughout this literature. We restate them because Section 9 rests on them and because the numerics there are stated in this notation; the proofs are included for self containedness and are short, not because they are new. Attributions are given after each statement.

Rearranging (7) as $a\,U f' = f(\mathcal{H}f - 1)$ gives

$$\frac{f'}{f} = \frac{\mathcal{H}f - 1}{a\,U}, \tag{10}$$

so f can only be singular where U vanishes.

Proposition 6 (Local exponent, [17])**.** *Let $U(y_*) = 0$ with $U'(y_*) = c \neq 0$. Then $f(y_*) = 0$, and $f \sim C\,(y - y_*)^\mu$ with*

$$\mu = \frac{c-1}{a\,c}. \tag{11}$$

Proof. Evaluating $a\,U f' = f(\mathcal{H}f - 1)$ at y_* gives $0 = f(y_*)\,(c-1)$, so $f(y_*) = 0$ unless $c = 1$. Expanding $U(y) = c\,(y - y_*) + O((y-y_*)^2)$ and using $U' = \mathcal{H}f$, so that $\mathcal{H}f(y_*) = c$, equation (10) becomes $f'/f = \mu/(y - y_*) + O(1)$ with μ as stated, and integrating gives the claim. □

Equation (11) is Theorem 1 of [17]. He states it as $\alpha(a) = \big(c_\omega + (1-a)\mathcal{H}\omega_a(\pi)\big)/\big(a\,\mathcal{H}\omega_a(\pi)\big)$, where α is the Hölder exponent of the *derivative* of the profile at the singular stagnation point, so the exponent of the profile itself is $1 + \alpha$; putting $c_\omega = -1$ and $\mathcal{H}\omega_a(\pi) = c$ gives $1 + \alpha = (ac - 1 + c - ac)/(ac) = (c-1)/(ac)$, which is (11). He also proves in the same theorem that the profile is C^1 but not $C^{1,\alpha}$ there, which is the regularity statement of this section, and that the frozen profile exists and is nonlinearly stable for a near 1. We obtained (11) independently and before finding [17]; the result is his.

The same computation applies to a narrowing profile. Since the narrowing regime is where most of this family lives, and since it is the case that can be tested against an exact solution, we state it in full rather than as an aside.

Proposition 7 (Local exponent, general self similar form)**.** *Let $\omega = (T-t)^{c_\omega}\bar{\Omega}\big(x/(T-t)^{c_l}\big)$, so that the profile equation is*

$$(c_l X + a\,\bar{U})\,\bar{\Omega}_X = (c_\omega + \bar{U}_X)\,\bar{\Omega}, \tag{12}$$

and let X_* be a zero of the total advection velocity $c_l X + a\bar{U}$, which replaces $\bar{U}$ as the transported quantity. Write $h = \mathcal{H}\bar{\Omega}(X_*) = \bar{U}_X(X_*)$ and suppose $c_l + a\,h \neq 0$. Then $\bar{\Omega}(X_*) = 0$ unless $h = -c_\omega$, and $\bar{\Omega} \sim C\,(X - X_*)^\nu$ with

$$\nu = \frac{c_\omega + h}{c_l + a\,h}. \tag{13}$$

If in addition the zero is simple, that is $\nu = 1$, then

$$h = \frac{c_l - c_\omega}{1-a}, \tag{14}$$

which for $c_\omega = -1$ reads $h = (1 + c_l)/(1-a)$.

Proof. Evaluating (12) at X_* annihilates the left hand side, leaving $0 = (c_\omega + h)\,\bar{\Omega}(X_*)$, so $\bar{\Omega}(X_*) = 0$ unless $h = -c_\omega$. Differentiating the advection velocity gives $(c_l X + a\bar{U})_X = c_l + a\,\bar{U}_X$, which equals $c_l + a\,h$ at X_*, so $c_l X + a\bar{U} \sim (c_l + a\,h)(X - X_*)$ there. Dividing (12) by $\bar{\Omega}$ and by the advection velocity gives $\bar{\Omega}_X/\bar{\Omega} = \nu/(X - X_*) + O(1)$ with ν as stated, and integrating gives the claim. For (14), setting $\nu = 1$ in (13) gives $c_\omega + h = c_l + a\,h$, that is $h(1-a) = c_l - c_\omega$. □

Proposition 6 is the case $c_l = 0$, $c_\omega = -1$, which is what a frozen profile requires: no spatial rescaling, and Proposition 8 below is the same case of (14).

Equation (14) is not new. [21] derives $\mathcal{H}\Omega(0) = (1+c_l)/(1-a)$ by the same argument, differentiating the profile equation at the stagnation point under the same nondegeneracy $\Omega'(0) \neq 0$, and records the slope $c_l + a\,\mathcal{H}\Omega(0)$ used in the proof above; we obtained it independently and state it here only because Proposition 6 is the case it does not cover. The content that remains with us is the exponent at a stagnation point where the zero is *not* simple, which is the situation at the second stagnation point on the circle and the one that fixes the spectral decay in Section 9. Section 8 checks the c_l dependence where $c_l \neq 0$ and the answer is known exactly.

Since $|y|^{\mu}$ has Fourier coefficients decaying like $k^{-(\mu+1)}$, the spectral decay exponent of the profile is

$$\beta = 1 + \frac{c-1}{a\,c}. \tag{15}$$

One local number therefore predicts the entire spectral decay rate.

Proposition 8 (Exact value at a simple zero)**.** *If in addition f has a simple zero at y_*, that is $f'(y_*) \neq 0$, then*

$$c = \frac{1}{1-a}. \tag{16}$$

Proof. Write $f \sim A(y - y_*)$ with $A = f'(y_*) \neq 0$, $U \sim c(y - y_*)$ and $\mathcal{H}f \sim c$. Matching the coefficient of $(y - y_*)$ in $a\,U f' = f(\mathcal{H}f - 1)$ gives $a\,c\,A = A\,(c-1)$, and dividing by A yields $ac = c - 1$, that is $c = 1/(1-a)$. □

This identity is standard in this literature, where it is generally used as a normalisation rather than derived. [17] imposes $c_\omega(t) = (a-1)u_x(t,0)$ as the gauge fixing the time rescaling, which at $c_\omega = -1$ is (16); [16] states the general form as $c_l = c_\omega + (1-a)U_X(0)$ in its equation (2.10); [21] states it as $\mathcal{H}\Omega(0) = (1+c_l)/(1-a)$; and Theorem 1 of [19] reaches $\gamma = 1/(1-a)$ for the complex singularity exponent from the same balance $a\gamma = \gamma - 1$. We claim none of it. What matters here is only that c at this stagnation point is known in closed form, which is what makes the control variate of Section 9 possible.

Equivalently $\mu = 1$ at such a point. Numerically, at $N = 4096$, the measured deviation of μ from 1 is -1.7×10^{-15}, -4.6×10^{-14}, -2.0×10^{-10} and 3.5×10^{-8} at $a = 0.70, 0.72, 0.74, 0.76$. The growth of this deviation at larger a tracks the profile's own accuracy, which degrades as the second exponent falls toward one. That the identity holds to machine precision on the discrete profile is what the control variate exploits.

Two stagnation points, exactly π apart. Numerically U has exactly two zeros, shown with the profile in Figure 5, and their separation is π to within 9×10^{-16} for every a tested. This needs no argument beyond the symmetry of the initial datum. Oddness is preserved by (2): if ω is odd about a point then $\mathcal{H}\omega$ is even about it, hence u is odd about it, hence both $u\omega_x$ and $u_x\omega$ are odd about it. Our datum $\omega_0 = \sin x$ is odd about 0 and about π, so the solution is odd about both for all time, so U vanishes at both for all time, and two points antipodal on the circle are π apart. The profile inherits this: scanning for a point about which f is odd, by minimising $\left\|\mathrm{Re}[\hat{f}_k e^{iky_0}]\right\| / \left\|\hat{f}_k\right\|$, returns a residual of 1.4×10^{-13} at $a = 0.8$ located at $y_0 = 0.975612$, which is y_1 itself, and 10^{-13} or smaller at $a = 0.75, 0.78, 0.82$. An earlier version of this paper gave a Fourier parity argument for the π separation and checked that f does not have only odd modes, $\left|\hat{f}_2\right| = 3315$ against $\left|\hat{f}_1\right| = 6520$. That check is beside the point: oddness about a shifted point is far weaker than having only odd modes, and the profile has it. The construction of [17] takes the profile odd from the outset.

Regularity of the profile. At $a = 0.8$ the second stagnation point has $\mu \approx 2$, and the general solution of (10) near a regular singular point permits different constants on the two sides. We find f'' bounded and exactly odd about y_2 to 10^{-9}, equal to $+2.27045$ on one side and -2.27045 on the other, a jump of 4.54089 with $C_+ = -C_- = 1.13522$. The profile is therefore $C^{1,1}$ but not C^2. It is not a logarithm: fitting $f'' = 2D \log |y - y_2| + \text{const}$ returns a slope of 0.043 at $R^2 = 0.46$, consistent with zero. Correspondingly f' is continuous at both stagnation points, to 4×10^{-12} and 1.6×10^{-11}.

8 An exact test at $a = 1/2$

Every measurement reported above was taken on a frozen profile, where $c_l = 0$ and (13) cannot be told apart from (11). This section checks the c_l dependence directly, because (2) is solvable in closed form at $a = 1/2$. Nothing in the section is claimed as new: the exact solution is from [20], the exponent $c_l = 1/3$ at $a = 1/2$ is stated in [19] and again in [20], and (14) is from [21]. It is included because the three fit together into a consistency check which is exact rather than numerical, and because the blowup time it produces for our datum does not appear in any of them.

Silantyev, Lushnikov, Siegel and Ambrose [20] construct exact pole dynamics solutions of (2) on the circle for $a = 0$ and $a = 1/2$. In the variable $X = \tan(x/2)$, which maps $(-\pi, \pi)$ onto $\mathbb{R}$, their $a = 1/2$ solution is a conjugate pair consisting of one double and one simple pole, whose amplitudes are tied by $\omega_{-1} = 2iv\, \omega_{-2}/(1 - v^2)$; that constraint is what cancels the logarithmic singularities which advection otherwise generates out of poles. The initial datum used throughout this paper lies in their class, since partial fractions give

$$\sin x \;=\; \frac{2X}{1 + X^2} \;=\; \frac{1}{X - i} + \frac{1}{X + i}, \tag{17}$$

a single conjugate pair at $v = 1$. That is the limit in which the complex singularity sits at infinite height, as it must for an entire datum, and it is the one point at which their parametrisation degenerates: the constraint reads $1 = (2i/0) \cdot 0$ there. The degeneracy is removable, and clearing it gives the following, which is a specialisation of [20] rather than a new solution.

Proposition 9 (Blowup time at $a = 1/2$)**.** *For $a = 1/2$ and $\omega_0 = \sin x$, the solution of (2) blows up at*

$$T \;=\; \pi \tag{18}$$

exactly, with the complex singularity reaching the real axis at $x = \pm\pi$.

Proof. The constraint forces $\omega_{-2,i}(0) = (v^2(0) - 1)/(2v(0))$, and substituting this into the coefficient of the pole equation of [20] cancels the vanishing denominator against the vanishing amplitude, leaving $K = 1/[2(v^2(0) + 1)^2]$, which is finite and equal to $1/8$ at $v(0) = 1$. The pole position therefore satisfies the regular equation

$$\frac{dv}{dt} = \frac{(v^2 + 1)^3}{32\, v^2}, \qquad v(0) = 1. \tag{19}$$

Set $G(v) = v(v^2 - 1)/(v^2 + 1)^2 + \arctan v$, so that $G'(v) = 8v^2/(v^2 + 1)^3$ and (19) integrates to $G(v(t)) = G(1) + t/4$. The right hand side of (19) is positive, so v increases and blowup occurs as $v \to \infty$, which is the pole reaching the real axis at $x = \pm\pi$. Since $G(1) = \pi/4$ and $G(\infty) = \pi/2$, $T = 4\big[G(\infty) - G(1)\big] = \pi$. $\square$

Taking $v \to \infty$ in the closed form near $x = \pi$, with $z = x - \pi$ and $\zeta = vz/2$, and using $dv/dt \sim v^4/32$ so that $v^3 = 32/(3(T-t))$, yields a self similar profile in the sense of Proposition 7 with

$$c_l = \tfrac{1}{3}, \qquad c_\omega = -1, \qquad \bar{\Omega}(\zeta) = -\frac{16}{3}\,\frac{\zeta}{(1+\zeta^2)^2}, \tag{20}$$

whence $\mathcal{H}\bar{\Omega} = -\frac{8}{3}(\zeta^2 - 1)/(\zeta^2+1)^2$ and $\bar{U} = \frac{8}{3}\,\zeta/(\zeta^2+1)$. The value $c_l = 1/3$ is not deduced here for the first time: it is the exponent $\alpha = 1/3$ recorded at $a = 1/2$ in [19], where it also arises as the exact value of their approximation $\alpha_0 = 2/(\gamma(\gamma+1))$ at $\gamma = 2$, and it is restated in [20] for both of their blowup types. The computation above merely confirms that our datum sits on the same branch. The total advection velocity is

$$c_l\zeta + a\bar{U} \;=\; \frac{\zeta}{3}\,\frac{\zeta^2+5}{\zeta^2+1}, \tag{21}$$

whose only zero is $\zeta = 0$, the blowup point itself, and $\bar{\Omega}$ has a simple zero there. Proposition 7 then predicts $h = (1+c_l)/(1-a) = (4/3)/(1/2) = 8/3$, against $1/(1-a) = 2$ for a frozen profile. The two differ by a third, so the test discriminates.

Measuring $h = (T-t)\,\mathcal{H}\omega(\pi,t)$ directly on the exact solution, with $T - t = 4[G(\infty) - G(v)]$ and the same spectral Hilbert transform used everywhere else in this paper, gives Table 5. The residual of the profile equation (12) for (20) is 1.3×10^{-15}, and $v^3(T-t) \to 32/3$ confirms $c_l = 1/3$.

v	10	30	100	300	1000
h measured	2.671992	2.667259	2.666720	2.666673	2.6666671
$\lvert h - 8/3\rvert$	5.3×10^{-3}	5.9×10^{-4}	5.3×10^{-5}	5.9×10^{-6}	4.5×10^{-7}
$\lvert h - 2\rvert$	6.7×10^{-1}	6.7×10^{-1}	6.7×10^{-1}	6.7×10^{-1}	6.7×10^{-1}

Table 5: The general form of Proposition 7 against the exact $a = 1/2$ solution, at resolutions $N = 2^{14}$ to 2^{20}. The measurement converges on $(1+c_l)/(1-a) = 8/3$ and stands off the frozen value $1/(1-a) = 2$ by two thirds at every resolution.

The same exercise calibrates Table 2. That table measures $c_l = 0.325$ at $a = 0.5$ against the exact $1/3$, a shortfall of 2.5 percent, while at $a = 0$, where $c_l = 1$ exactly, it returns 1.048 to 1.058. The error is therefore a few percent and is not of one sign, which is what the fuller comparison against the published branch in the introduction already showed, and what makes the withdrawn estimate of a_c untenable.

Finally, $\bar{\Omega}$ in (20) is analytic on $\mathbb{R}$, its nearest singularities being at $\zeta = \pm i$. The $C^{1,1}$ regularity and the algebraic spectral decay (15) found in Section 7 are thus features of the frozen regime specifically, not of blowup in this family generally. That is consistent with Proposition 7: with $c_l > 0$ the total advection velocity has a nonzero slope $c_l + ah$ at the stagnation point even when $\bar{U}$ alone would vanish to higher order, so the regular singular point is milder.

9 Determination of the global constant

Proposition 8 pins the stagnation point at which the profile is smooth, and which therefore contributes no singularity. The exponent β is set by the other one, whose c, written c_2 below, is genuinely global: no local balance determines it.

Reading c_2 off a single grid is unreliable. Across $N = 512$ to 4096 it wanders between -1.6486 and -1.6681 without a monotone trend, and a three parameter fit of the form $c_2(N) = c_2^\infty + AN^{-p}$ returns $p = 3.3$ with amplitude 1.1×10^7, which is a fit to noise. The reason is the $C^{1,1}$ regularity established above: every quantity read from the profile converges algebraically.

The remedy is that c_1 is known exactly. Both constants are read from the same profile and carry the same discretisation error, entering linearly, so c_2 is a linear function of c_1 across resolutions and evaluating that line at the exact c_1 cancels the error without requiring its size or its rate. At $a = 0.8$ the regression over seven resolutions is

$$c_2 = -0.980361\, c_1 + 3.240505, \qquad R^2 = 0.99999744, \tag{22}$$

and the raw spread of 1.95×10^{-2} collapses to 2.43×10^{-5}, a factor of 801. The corrected value from $N = 512$ then lies within 1.5×10^{-5} of that from $N = 4096$. We obtain

$$c_2 = -1.66130027 \pm 1.0 \times 10^{-5}, \quad \mu_2 = 2.00242268, \quad \beta = 3.00242268. \tag{23}$$

a	c_2	scatter	μ_2	β
0.70	-0.10252834	4.1×10^{-16}	15.36200	16.36200
0.71	-0.20450843	6.0×10^{-16}	8.29546	9.29546
0.72	-0.31519119	1.4×10^{-14}	5.7953854	6.7953854
0.74	-0.56651088	4.2×10^{-10}	3.7367448	4.7367448
0.76	-0.86560395	1.8×10^{-8}	2.8358720	3.8358720
0.78	-1.22477889	1.3×10^{-6}	2.3288127	3.3288127
0.80	-1.66130509	1.2×10^{-5}	2.0024205	3.0024205
0.82	-2.20024724	5.3×10^{-5}	1.7737736	2.7737736

Table 6: The global constant and the resulting exponents. The scatter is the spread of the corrected values across resolutions and measures self consistency, not residual systematic error. The rows at $a = 0.70$ and $a = 0.71$ were computed over $N = 1024$ to 3072 rather than the full ladder, and are quoted to the digits that run resolves.

Remark 10 ($\beta \neq 3$)**.** The value $\mu_2 = 2$, and hence $\beta = 3$, would require $c_2 = 1/(1 - 2a) = -1.66666667$ at $a = 0.8$. The corrected value misses this by 5.37×10^{-3}, some five hundred times the scatter of the corrected points. Since the correction removes eight hundred times the raw error, the conclusion survives allowing a residual systematic an order of magnitude above the observed scatter. Table 6 shows β varying continuously with a; the value 3 is merely where that curve crosses.

Remark 11 (Against the published exponent)**.** [19] measure this same exponent for the frozen profile, calling it p_b, by a two domain least squares fit to the spectrum, and report $p_b = 9.32592$ at $a = 0.71$. Equation (15) with c_2 from Table 6 gives $\beta = 9.29546$ there, lower by 0.03046, or

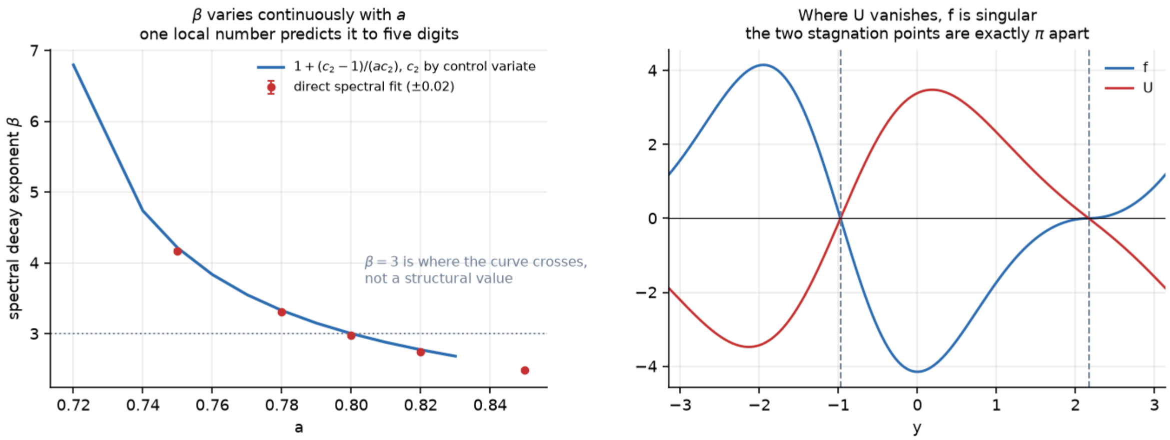

Figure 5: Left: the spectral decay exponent β against a, from (15) with c_2 fixed by the control variate. The curve is smooth and $\beta = 3$ is simply where it crosses. Direct fits of $\left|\hat{f}_k\right| \sim k^{-\beta}$ to the spectrum are shown for contrast with error bars of ± 0.02, which is their window sensitivity; the relation is four orders of magnitude more accurate than measuring the exponent directly. Right: the profile f and its velocity U at $a = 0.8$. The dashed lines mark the two zeros of U, which are exactly π apart, and f vanishes at both as Proposition 6 requires.

0.33 percent. The two determinations share nothing: theirs is a fit to the tail of the spectrum over a window, ours is a single value of $\mathcal{H}f$ read off the profile at a point. Given the window sensitivity documented in the next remark we read the difference as a correction to the fitted value rather than a disagreement, and we claim no more than the three digits it rests on.

Their exponent diverges as $a \to a_c^+$, and β here does the same, which gives an independent handle on a_c. Extrapolating $1/\beta$ linearly to zero from the pairs $(0.70, 0.71)$ and $(0.71, 0.72)$ gives 0.6868 and 0.6828, with the pair nearer the transition returning the larger value, pointing at their $a_c = 0.6890665337007457\ldots$ and not at anything larger. This is an extrapolation through convex data, so we quote it for its direction only, but that direction is what withdraws the estimate of a_c discussed in the introduction.

Remark 12 (The correction rests on one anchor)**.** The correction uses a single exactly known quantity, and we were unable to validate it against a second. The only other constant available in closed form on this profile is the constraint of Section 10, and that one holds by symmetry rather than by accuracy, so it carries no discretisation error and cannot anchor anything. The evidence that the correction is doing what it claims is therefore internal: the corrected values from six resolutions collapse onto one number, the raw spread falling by a factor of 800, and $N = 512$ lands within 1.5×10^{-5} of $N = 4096$ once corrected. That is consistency across resolutions, not agreement with an independent determination, and it does not exclude a systematic common to every resolution. A second anchor, in this problem or another, would be the natural next test.

Remark 13 (On measuring β from the spectrum directly)**.** We caution against it. Fitting $\left|\hat{f}_k\right| \sim k^{-\beta}$ over a band is sensitive to the band at the 2×10^{-2} level: shifting the window from $128 \le k \le 512$ to $0.094\, k_{\mathrm{cut}} \le k \le 0.375\, k_{\mathrm{cut}}$, the same window to three digits, moves the answer from 3.00315 to 2.98626. Across ten reasonable windows a binned estimator spans 2.9829 to 3.0072 and an unbinned least squares fit spans 3.0132 to 3.0510, and the two barely overlap. The two ends of the spectrum are biased in opposite directions: the low end by the analytic factor multiplying $|y - y_*|^\mu$, which contributes $k^{-(\mu+2)}$ and faster, and the high end by the dealiasing mask. Refinement distinguishes them, since the former is pinned to absolute k and the latter to a fixed fraction of k_{cut}. Equation (15) with a well determined c_2 is four orders of magnitude more accurate than any of these fits.

10 A first integral and a global constraint

Equation (10) integrates in closed form. On any interval free of zeros of U,

$$f = C\ |U|^{1/a} \exp\Big(-\frac{1}{a}\int \frac{\mathrm{d}y}{U}\Big). \tag{24}$$

Near a simple zero this yields $|y - y_*|^{1/a}\,|y - y_*|^{-1/(ac)} = |y - y_*|^\mu$, recovering Proposition 6 independently.

Proposition 14 (Global constraint). *If f and U are 2π periodic and $\log|f|$ has no jump at either zero of U, then*

$$\mathrm{PV}\oint \frac{\mathrm{d}y}{U} = 0. \tag{25}$$

Proof. Integrating (10) once around the circle, $0 = \frac{1}{a}\big[0 - \mathrm{PV}\oint \mathrm{d}y/U\big]$, since both $\log|f|$ and $\log|U|$ return to their initial values. □

The hypothesis holds here: at y_1 the profile is smooth with $\mu = 1$, and at y_2 the one sided constants satisfy $C_+ = -C_-$, so $|C_+| = |C_-|$ and the logarithm does not jump. We verify (25) by subtracting both simple poles with cot, which carries the same residue and whose own principal value on the circle vanishes. The resulting ratios are 2.2×10^{-12}, 6.7×10^{-13}, 9.8×10^{-13} and 1.4×10^{-12} at $a = 0.75, 0.78, 0.80, 0.82$, stable across three independent grid shifts.

That verification is weaker than it looks. For the profile studied here (25) holds by symmetry, independently of the profile equation. Section 7 records that f is odd about y_1; hence $\mathcal{H}f$ is even about y_1, hence U is odd about it, measured as $\max|U(y_1+s) + U(y_1-s)|\,/\,\|U\|_\infty = 3.7 \times 10^{-14}$ at $a = 0.8$, $N = 2048$. An odd integrand has vanishing principal value on the circle by antisymmetry alone. Consistently, the computed value of $\mathrm{PV}\oint \mathrm{d}y/U$ does not improve with resolution: across $N = 512$ to 3072 at $a = 0.8$ it wanders between 8.4×10^{-14} and 8.9×10^{-13} with no trend and changing sign, while over the same ladder the error in c_1 falls monotonically from 1.3×10^{-2} to 2.2×10^{-3}. So the quantity carries no discretisation error and its agreement with zero measures the symmetry of the datum rather than the accuracy of the solve. Proposition 14 is not thereby weakened as a statement, since it assumes no symmetry and would have content for a profile that is not odd, but it is untested by this computation, and it cannot serve as an independent anchor for the control variate of Section 9.

Relation to the orbit invariants at $a = 1$. A principal value integral of this shape is not new to the model. At $a = 1$, where (2) becomes the Lie bracket form $\omega_t + [u, \omega] = 0$ and the dynamics is motion on an adjoint orbit of $\mathrm{Diff}_+(S^1)$, Jia, Stewart and Šverák [4] identify $b = \text{p.v.} \int_{S^1} \mathrm{d}\theta/\omega_0(\theta)$ as an orbit invariant in their equation (2.14), and observe that its conservation, together with the conservation of ω_θ at the zeros of ω, is an analogue of the Kelvin, Helmholtz law. Equation (25) is a different statement: the integrand carries the velocity rather than the vorticity, the setting is the frozen profile at $a \approx 0.8$ rather than the $a = 1$ dynamics, and the content is that the integral vanishes rather than that it is conserved. The orbit structure they use is special to $a = 1$, the only member of the family that is a pure Lie bracket, and does not survive $a \neq 1$. The two are nonetheless close enough in shape that we claim nothing for the form of (25), only for its value and for its derivation from (10). We record separately that the conserved quantity of Lei, Liu and Ren [5], the H^1 norm of $\sqrt{\omega}$ for one signed data, is unrelated to either.

Remark 15. A naive evaluation of (25) on the grid returns ratios between 10^{-2} and 1 and appears to refute it. This is catastrophic cancellation: the stagnation points land on grid points to within 10^{-11} of a cell, so the subtraction differences two quantities of size 10^8. Evaluating on a half shifted grid, which is exact for a band limited field, resolves it.

No closed form for c_2. With c_2 determined across eleven values of a, candidate shapes can be excluded rather than merely left unconfirmed. Every Möbius form is rejected: $\mu_2 = (p+qa)/(1+ra)$ leaves an rms residual of 1.9×10^{-4}, $c_2 = (p+qa)/(1+ra)$ leaves 3.0×10^{-4}, and the same shape in the variable $1/(1-a)$ leaves 6.0×10^{-4}, each one to two orders above the data's precision. Fits of quadratic over quadratic achieve residuals of order 10^{-7} but use five parameters against eleven points and dip below the data scatter at the rough end of the range, so they absorb smooth error rather than signal and we do not regard them as evidence.

We suggest this is the correct answer rather than a gap. Proposition 8 succeeds because it is a *local* balance at a point where f is smooth. No such balance is available at the second stagnation point, so its value is determined by the global solution. Writing ψ for the positive frequency part of U, so that $U = \psi + \bar{\psi}$ and $f = i(\psi' - \bar{\psi}')$, equation (7) reads

$$a\,(\psi + \bar{\psi})(\psi'' - \bar{\psi}'') = (\psi' - \bar{\psi}')(\psi' + \bar{\psi}' - 1), \tag{26}$$

and the mixed products $\psi\bar{\psi}''$ and $\bar{\psi}\psi''$ straddle both halves of the spectrum. That failure to separate is exactly what makes $a = 0$ integrable and $a \neq 0$ not.

11 Limitations

The datum $\sin x$ is not generic: it is precisely the ground state of the $a = 1$ model. Table 4 answers the worst form of this objection, reaching the same profile from sixteen random data and from a continuous family of offsets, always with the same constants to seven digits. It does not map the basin, and an earlier version of this paper contained a section which probed its boundary along two one parameter families and found a window of data decaying like $1/t$ rather than blowing up. That material is not needed for the determination of β and has been removed; it remains in the repository.

All statements about $a = 0.9$ and above are unresolved. The residual of the profile equation there does not fall monotonically with the amplitude cap, taking values 0.78, 2.93, 1.77 at caps

10^4, 10^6, 10^8, so those measurements reflect the fitting window rather than the solution. Since $T(0.9) \approx 10.8$ against 6.1 at $a = 0.8$, comparisons should be made at a fixed fraction of T rather than a fixed amplitude.

The scatter quoted in Table 6 measures how consistently the control variate reproduces itself across resolutions. A residual nonlinear dependence of the discretisation error on c_1 would cancel from it and go undetected, so the figure of 1.4×10^{-14} at $a = 0.72$ should not be read as fourteen digit accuracy.

On priority. The bibliographic details of every reference above have been verified. Twelve closely related works have been read for overlap: [3], [11], [12], [13], [14], [15], [16], [19], [20], [21], [17] and [18]. The honest summary is that this is a numerical note about a constant, in a setting other people built.

We claim none of the following. The two regime picture on the circle, the critical advection a_c, the frozen blowup $\omega = f(x)/(T-t)$ and its numerical profile, the derivative jump at the antipodal point, the algebraic spectral decay it causes, and stability as inferred from converging simulations, are all in [19]. Existence and nonlinear stability of the frozen profile for a near 1, the local exponent (11), and the C^1 but not $C^{1,\alpha}$ regularity at the singular stagnation point are Theorems 1 and 2 of [17]. Equation (14) and hence Proposition 7 appear in [21] and, as equation (2.10), in [16], and Proposition 8 is the normalisation [17] imposes to fix the time rescaling. The exact $a = 1/2$ solution of Section 8 is from [20], and Proposition 9 is a specialisation of it. We derived several of these relations independently before finding the references, which is a fact about how the work went and not a claim on it.

What we claim is the control variate of Section 9 and what it yields: β to five digits, the exclusion of $\beta = 3$ at $a = 0.8$, and the correction to the fitted exponent of [19] recorded in Remark 11; the linear spectrum of Section 6 at $a = 0.8$, which is numerical where [17] is a theorem near $a = 1$; and the first integral and global constraint of Section 10, with the qualification recorded there. We did not find either in [17], [16] or the pole dynamics papers, but a principal value integral of a reciprocal with simple zeros, serving as a global invariant, is already in [4] at $a = 1$; (25) concerns a different field in a different setting and says the integral vanishes rather than that it is conserved, but we claim nothing for its shape. Both are elementary consequences of separating (10) and we would not be surprised to be shown they are known.

This reference list grew four times while being compiled, and that history is the strongest caveat we can offer. [19], [20], [21] and [18] belong to a line of work using complex singularity and pole dynamics methods which searches organised around the other references do not surface, and it is the line that works on the circle. [17] was found later still, through a citation inside [18] which turned out to describe it inaccurately. We have read [19] in full and [17] and [21] in part, and for the preprints this rests on a reading of the text rather than a line by line verification of every lemma. Both numerical coincidences with [16] have been examined; neither is an overlap, and the first, the exchange of stability near $a \approx 0.75$, is to be compared against $a_c = 0.68907$ rather than against the estimate withdrawn above, and remains unsettled.

The critical limit $a \to 1$ is left open and is not treated here. An earlier version of this paper reported no exponent for $T(\varepsilon)$ because the measured one does not converge over the range we can reach, and argued that the shortfall cannot be made up by analysis in place of computation, the linearisation at $a = 1$ having purely imaginary spectrum with the equilibrium manifold in its kernel and therefore no spectral gap to reduce onto. That material is independent of everything above and has been removed; it remains in the repository.

Finally, nothing here is a proof. A computer assisted proof in this setting, in the style of Chen and Hou [9], requires interval arithmetic producing certified enclosures rather than floating point with convergence studies. The objects this paper produces, a profile equation with a linearly stable solution and an exact relation fixing one of its two local constants, are the objects such a proof would need to enclose.

References

[1] P. Constantin, P. D. Lax and A. Majda, *A simple one dimensional model for the three dimensional vorticity equation*, Comm. Pure Appl. Math. **38** (1985), 715-724.

[2] S. De Gregorio, *On a one dimensional model for the three dimensional vorticity equation*, J. Statist. Phys. **59** (1990), 1251-1263.

[3] H. Okamoto, T. Sakajo and M. Wunsch, *On a generalization of the Constantin, Lax and Majda equation*, Nonlinearity **21** (2008), 2447-2461.

[4] H. Jia, S. Stewart and V. Šverák, *On the De Gregorio modification of the Constantin, Lax and Majda model*, Arch. Ration. Mech. Anal. **231** (2019), 1269-1304.

[5] Z. Lei, J. Liu and X. Ren, *On the Constantin, Lax and Majda model with convection*, Comm. Math. Phys. **375** (2020), 765-783.

[6] J. Chen, T. Y. Hou and D. Huang, *On the finite time blowup of the De Gregorio model for the 3D Euler equations*, Comm. Pure Appl. Math. **74** (2021), 1282-1350.

[7] G. Luo and T. Y. Hou, *Potentially singular solutions of the 3D axisymmetric Euler equations*, Proc. Natl. Acad. Sci. USA **111** (2014), 12968-12973.

[8] T. M. Elgindi, *Finite time singularity formation for $C^{1,\alpha}$ solutions to the incompressible Euler equations on $\mathbb{R}^3$*, Ann. of Math. **194** (2021), 647-727.

[9] J. Chen and T. Y. Hou, *Stable nearly self similar blowup of the 2D Boussinesq and 3D Euler equations with smooth data I: Analysis*, preprint, arXiv:2210.07191 (2022).

[10] J. Chen and T. Y. Hou, *Stable nearly self similar blowup of the 2D Boussinesq and 3D Euler equations with smooth data II: Rigorous numerics*, Multiscale Model. Simul. **23** (2025), 25-130.

[11] D. Huang, J. Tong and D. Wei, *On self similar finite time blowups of the De Gregorio model on the real line*, preprint, arXiv:2209.08232 (2022).

[12] D. Huang, X. Qin, X. Wang and D. Wei, *Self similar finite time blowups with smooth profiles of the generalized Constantin, Lax and Majda model*, preprint, arXiv:2305.05895 (2023).

[13] D. Huang, X. Qin and X. Wang, *Multi scale self similar finite time blowups of the Constantin, Lax and Majda model for the 3D Euler equations*, preprint, arXiv:2401.14615 (2024).

[14] F. Zheng, *Exactly self similar blow up of the generalized De Gregorio equation*, Nonlinearity **36** (2023), 5252-5264.

[15] J. Guo and Q. Jiu, *Stability and instability on the De Gregorio modification of the Constantin, Lax and Majda model*, preprint, arXiv:2506.02800 (2025).

[16] D. Huang, J. Tong and X. Wang, *Self similar finite time blowups with singular profiles of the generalized Constantin, Lax and Majda model: theoretical and numerical investigations*, preprint, arXiv:2603.25104 (2026).

[17] J. Chen, *On the slightly perturbed De Gregorio model on* S^1, Arch. Ration. Mech. Anal. **241** (2021), 1843-1869.

[18] D. M. Ambrose, P. M. Lushnikov, M. Siegel and D. A. Silantyev, *Global existence and singularity formation for the generalized Constantin, Lax and Majda equation with dissipation: the real line versus periodic domains*, Nonlinearity **37** (2024), 025004.

[19] P. M. Lushnikov, D. A. Silantyev and M. Siegel, *Collapse vs. blow up and global existence in the generalized Constantin, Lax and Majda equation*, J. Nonlinear Sci. **31** (2021), 82.

[20] D. A. Silantyev, P. M. Lushnikov, M. Siegel and D. M. Ambrose, *Exact periodic solutions of the generalized Constantin, Lax and Majda equation with dissipation*, Stud. Appl. Math. **155** (2025), e70115.

[21] J. Xu, *The spectral picture of self similar collapse in the Constantin, Lax and Majda equation*, preprint, arXiv:2607.19762 (2026).